CCD Characterization, Extinction Coefficients and Photometry of Open Cluster (Pleiades)

Observational Astronomy Lab
Project Report

by

Mahiguhappriyaprakash *

Supervised by
Prof. Harinder P. Singh

Submitted on May 7, 2024

* Examination Roll No. : 22222762128, Email: manjulaprakash2002@gmail.com

Table of Contents

List of Figures v

List of Tables v

Acknowledgement **vi**

1. Introduction **1**

2. Instruments Used **2**

2.1. Telescope 2

2.1.1. Light Gathering Power of a Telescope (Light Grasp(G_L)) 2

2.1.2. Magnitude Limit of the Telescope(L_{mag}) 3

2.1.3. Is our telescope slow or fast? 4

2.2. Charge Coupled Device (CCD) 4

2.2.1. Working Principle 4

2.2.2. Advantages of CCDs 5

2.2.3. Typical CCD System 6

2.2.4. Specifications 6

2.2.5. Field Of View 6

2.2.6. Quantum Efficiency 7

2.2.7. CCD Gain and Read Noise 8

2.3. Filter Wheel 9

3. Observations **10**

4. Data Analysis **11**

4.1. CCD Characterization 11

4.1.1. Imaging and Calibration: 11

4.1.2. Calculating Gain and Readout Noise: 13

4.2. Image reduction 15

4.3. Aperture Photometry of Pleiades Cluster 16

4.4. Extinction Coefficients 19

4.4.1. Airmass 20
4.4.2. Local Siderial Time (LST) 20
4.4.3. Calculation of LST and Airmass in Python 21
4.4.4. Extinction coefficient 22

5. Result and Conclusion **24**
5.1. Result 24
5.2. Conclusion 26

Appendices **27**

A Readout Noise and Gain Tables **27**

B Magnitudes and Extinction Coefficients of Star 3 and Star 4 **33**

C CCDSOFT **35**

D Log File **36**

E Astrophotography (Image Reduction) **43**

Bibliography **44**

List of Figures

1 Celestron CGE 1100 2

2 (a) 3D view of CCD (b) 2-D array depiction of CCD 5

3 CCD structure 5

4 Quantum Efficiency Of ST-7XME 8

5 Model IFW Intelligent Filter Wheel 9

6 The four stars of Pleiades under observation 11

7 Light Frame (Exposure Time: 0.1 sec , Open Filter) 11

8 Bias Frame (Exposure Time: 0.00 sec) 12

9 Dark Frame (exposure time: 0.001 sec) 12

10 Flat frame (exposure time: 0.5 sec, open filter) 13

11 Using imarith and imstat in IRAF 14

12 Gain in different filters 14

13 Table of various expressions calculated for determining gain (open filter). Other tables are available in Appendix A 14

14 An illustration of image reduction procedure using IRAF. 15

15 The sequence of stars considered during the observation. 17

16 List of datapar parameters whose values are to be set according to our star in observation 17

17 List of centerpars parameters whose values are to be set according to our star in observation 18

18 List of fitskypars parameters whose values are to be set according to our star in observation 18

19 List of photpars parameters whose values are to be set according to our star in observation 19

20 Curve of growth obtained for Alcyone in open filter. The instrumental magnitude turns out to be 6.84 19

21 Header file of a frame from open filter. Note that there are two keywords 'DATE-OBS' and 'TIME-OBS' which contains the UTC date and time of the frame. 21

22 Extinction coefficient in different filters for star 1 23

23 Extinction coefficient in different filters for star 2 24
24 Extinction coefficient in different filters for star 3 33
25 Extinction coefficient in different filters for star 4 34
26 Jupiter as viewed from Department of Physics and Astrophysics, University of Delhi 43
27 Orion Nebula as viewed from Department of Physics and Astrophysics, University of Delhi 43

List of Tables

1 Observations of Bias, Dark and Flat 10
2 Observations for Pleiades 10
3 Readout noise and gain 25
4 STAR 1 : Alcyone 25
5 STAR 2 : 24 TAURI 25
6 Here is an example of the selection of pairs 27
7 Readout noise for open filter 28
8 Readout noise for red filter 30
9 Readout noise for green filter 31
10 Readout noise for blue filter 32
11 STAR 3 : V647 TAURI 34
12 STAR 4 : HD 23608 35

Acknowledgement

I would like to express my heartfelt gratitude to the Astronomy Lab, Department of Physics and Astrophysics, University of Delhi, for granting me the opportunity to undertake this project and for generously providing the necessary equipment for the same.

Special thanks to Prof. Harinder P. Singh for his invaluable guidance and mentorship throughout this journey.

I am deeply thankful to Mr. Nitesh Kumar (SRF) for his unwavering support and assistance.

My sincere gratitude goes to my friends, Shahana Saifi and Sonali Saxena, for their constant help, without which this project could not have been completed.

1. Introduction

Initially, astronomers used qualitative terms like "bright" or "faint" to describe the brightness of a star, leading to a need for a quantitative measure. The concept of apparent magnitude was developed, assigning numerical values to stars' brightness as seen from Earth. This allowed for more precise comparisons and tracking of changes in brightness over time, such as those caused by variable stars. The magnitude scale provided a standardized way to describe brightness, essential for advancing our understanding of the universe.

Nowadays astronomers use two types of magnitudes: **apparent magnitude** and **absolute magnitude**. Apparent magnitude measures a star's brightness as seen from Earth, while Absolute Magnitude is the brightness a star would have if placed at a standard distance of 10 parsecs from Earth, describing its intrinsic luminosity.

This project focuses on determining the **apparent magnitude** of stars within the **Pleiades**, also known as *The Seven Sisters*. Located in the northwest of the Taurus constellation, the Pleiades is an open cluster of tens of thousands of young or middle-aged stars. Unlike globular clusters, which are densely packed and contain millions of old stars, open clusters like the Pleiades are loosely bound by gravitational attraction and have high metallicity.

Observing stars through telescopes presents challenges due to various noises and atmospheric effects. Images captured by **CCDs** for light through telescopes are initially raw and require processing to remove noise. We use the **IRAF** (*Image Reduction and Analysis Facility*) software package, specifically the **CCDRED** and **DIGIPHOT** packages, to reduce noise and perform photometry, respectively.

Photometry allows one to obtain the **instrumental magnitude** of stars, which is an uncalibrated apparent magnitude. To derive the **apparent magnitude**, one must calibrate images using **extinction coefficients**. These coefficients are determined by plotting the apparent magnitude against the air mass, providing a calibration factor to correct for atmospheric effects.

The goal of this project is to find the different characteristics of the CCD used and to study the brightness of stars in the Pleiades, which will help to learn more about the types of stars in this cluster.

2. Instruments Used

2.1. Telescope

The astronomical observatory of our department is equipped with a telescope of following specifications:

- Optical design: 11” Schmidt Cassegrain
- Focal length: 2800 mm
- Aperture Diameter: 280 mm
- Focal ratio: f/10
- Mount: Computerized Equatorial Mount
- Eyepiece: 40 mm plossl (1.25”)
- Star diagonal: 1.25”

Figure 1: Celestron CGE 1100

2.1.1. Light Gathering Power of a Telescope (Light Grasp(G_L))

The light gathering power of the telescope is proportional to the square of diameter of objective lens (D_o) of Telescope. i.e.

$$G_L \propto D_o^2 \tag{2.1}$$

Comparing light gathering power of an eye with the light gathering power of a telescope, we get

$$G_L = (\frac{D_o}{D_{\text{eye}}})^2 \tag{2.2}$$

times the light gathering power of eye

where, $D_{\text{eye}} = 7\text{mm}$, is the typical diameter of the pupil of a typical human eye.

So, we get

$$G_L = D_o^2 \times 2 \times 10^4$$

times the light gathering power of the eye

but,

$$D_o = 280 \text{ mm}$$

we get,

$$G_L = 1568 \tag{2.3}$$

times the light gathering power of the eye. So, a telescope of aperture of 280 mm can gather 1568 times more light than compared to a typical human eye.

The gain in terms of magnitude (G_{mag}) is given by

$$G_{\text{mag}} = 2.5 \times log(G_L) \tag{2.4}$$

Hence,

$$G_{\text{mag}} = 2.5 \times log(1568) = 7.9883 \tag{2.5}$$

This gives us the the amount of magnitude that telescope will let us see.

2.1.2. Magnitude Limit of the Telescope(L_{mag})

To find the faintest magnitude one can see with a telescope, we use the following relation:

$$L_{\text{mag}} = G_{\text{mag}} + L_{(\text{mag})\text{eye}} \tag{2.6}$$

where, $L_{(\text{mag})\text{eye}} = 6$ is the faintest magnitude our eyes can see.

Hence,

$$L_{\text{mag}} = 7.9883 + 6 = 13.9883 \tag{2.7}$$

Therefore, the faintest magnitude which can be observed from our telescope is = 13.9883

2.1.3. Is our telescope slow or fast?

Fast telescope is one with a smaller focal ratio. It is called fast because it produces a brighter image with more photons per pixel which results in shorter (or faster) exposures being needed to capture an image. Traditionally, telescopes with focal ratios of f/5.0 and below are considered fast.

A slow telescope is one with a larger focal ratio. It is called slow because it produces a dimmer image with fewer photons per pixel, which results in longer (or slower) exposures being needed to capture an image.Traditionally, telescopes with a focal ratio above f/8.0 are considered slow.

Since our telescope has the focal ratio is f/10, we would call it a **slow telescope**.

2.2. Charge Coupled Device (CCD)

CCD detectors are 2-D arrays of detection elements (or pixels) that convert incident photons into electronic charge , it is widely used for optical digital imaging in astronomy.

2.2.1. Working Principle

The working principle if CCD is mainly based on the photoelectric effect. When a photon is absorbed in the silicon, it generates a photoelectron. This photoelectron is then free to move under the influence of an electric field. However, for imaging purposes, it is crucial that the photoelectron does not wander away from the point where it was created by the photon impact. This is achieved by applying a special electrostatic field that attracts the photoelectrons to a specific spot and by creating storage wells. These storage wells are formed by applying metal electrodes to the silicon, along with a thin insulating layer of SiO_2 (0.1μ in thickness). The process of extracting the photogenerated charge, and thus the image, is known as charge coupling.

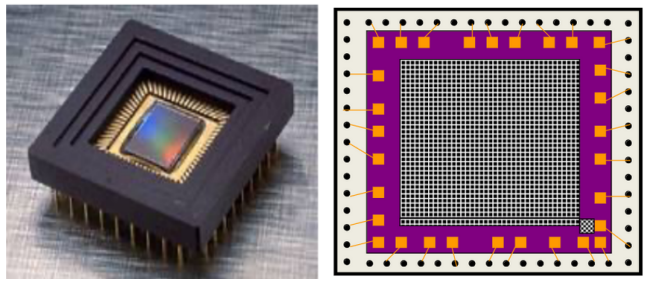

Figure 2: (a) 3D view of CCD (b) 2-D array depiction of CCD

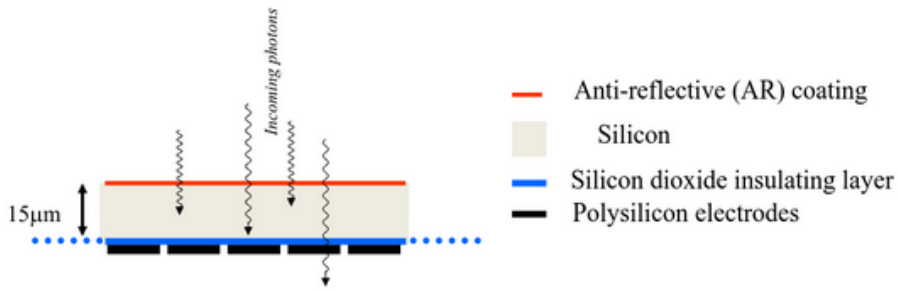

Figure 3: CCD structure

2.2.2. Advantages of CCDs

- Revolutionized astronomical observations
- Linear Devices
- High Quantum Efficiency
- Gain of almost 100 times
- The increase in QE over film is like making a telescope into a much bigger one – effectively allowing a 1-m telescope to perform like a 4-m.
- Large spectral range (0.3 microns to 1 microns)
- The accuracy of CCDs in both linearity and stability means the measurements made are of the highest quality, and a wider band of the spectrum is utilized.

2.2.3. Typical CCD System

Camera Head

- CCD Detector
- Cooling system (Thermo-electrically or cryogenically cooled)

Camera Electronics

- Signal processing hardware
- Analogue to Digital Converter
- Timing Logic
- Electronic interface to computer

Computer

- Needed to communicate with the CCD
- Image acquisition software
- Image Processing Software (MIDAS, IRAF)
- Normally UNIX/LINUX operating system required

2.2.4. Specifications

Model: ST-7XE/XME

CCD used: Kodak KAF-0402E/ME + TC-237

Number of Pixels: 765×510 pixels

Pixel Dimensions: 9×9 microns

Array Dimensions: 6.9×4.6 mm

2.2.5. Field Of View

Focal ratio: (f/ratio)

where, ratio = $\frac{FocalLengthoftheAperture}{ApertureDiameter}$

So, ratio = $\frac{2800}{280}$ = 10

Therefore,

$$\textbf{focal ratio} = f/10 \tag{2.8}$$

Plate scale:

p = $\frac{1}{f}$

and s = f $\times\theta$

where, s = size of image on focal plane, θ = angular size of image

p=$\frac{\theta}{s}$ = ($\frac{206265}{2800}$)"/mm

$\Longrightarrow$

$$\textbf{plate scale} = 74''/mm \tag{2.9}$$

Now, chip size = (765 × 0.009)mm × (510 × 0.009)mm

$\Longrightarrow$

$$\textbf{chip size} = 6.885mm \times 4.59mm \tag{2.10}$$

Field of view (FOV):

FOV = plate scale × chip size

= (6.885 × 74)" × (4.49 × 74)"

=(509.49)" × (339.66)"

$\Longrightarrow$

$$\textbf{Field of view of the CCD} = 8.49' \times 5.66' \tag{2.11}$$

2.2.6. Quantum Efficiency

The quantum efficiency of a CCD represents its photovoltaic response, indicating the number of electron-hole pairs generated and correctly read out by the device for each incident photon. Not every photon that reaches the detector will be detected and converted into an electrical signal. The

Quantum Efficiency (QE) is the percentage of photons that are detected. For instance, the human eye has a QE of approximately 20%, photographic film around 10%, and high-performance CCDs can exceed 80%. The QE is wavelength-dependent.

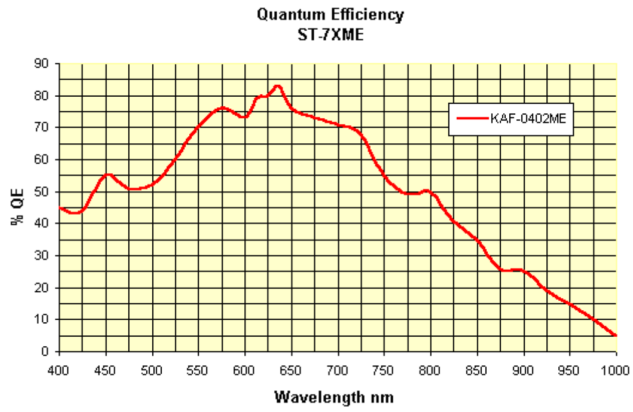

Figure 4: Quantum Efficiency Of ST-7XME

2.2.7. CCD Gain and Read Noise

GAIN: The gain of a CCD is set by the output electronics and determines how the amount of charge collected in each pixel will be assigned to a digital number in the output image. Gain values are usually given in terms of the number of electrons needed to produce one ADU step within the A/D converter.

READOUT NOISE: Readout noise is usually quoted for a CCD in terms of the number of electrons introduced per pixel into your final signal upon readout of the device. The readout noise consists of two inseparable components. First is the conversion from an analog signal to a digital number, which is not perfectly repeatable. Each on-chip amplifier and A/D circuit will produce a statistical distribution of possible answers centered on a mean value. Thus, even for the hypothetical case of reading the same pixel twice, each time with identical charge, a slightly different answer may be produced. Second, the electronics themselves will introduce spurious electrons into the entire process, which will produce unwanted random fluctuations in the output. These two effects combine to produce an additive uncertainty in the final output value for each pixel. The average level (one sigma) of this uncertainty is the read noise and is limited by the electronic properties of the on-chip output amplifier and the output electronic.

2.3. Filter Wheel

To take the observations we have made use of the Model IWF Intelligent Filter Wheel. The Optec IFW has the ability to determine the identification (ID) of a particular wheel and apply that wheel ID to a stored set of filter names. The names, not just position numbers of these filters, are displayed on the eight character display and are also available to the camera operating software via a RS-232 interface using a simple command structure. The IFW can be controlled by either the switches on the hand control, an SBIG camera controller (TTL level pulses), or by an external computer via a RS-232 interface. The RS-232 operating protocol is a set of simple ASCII commands that any programmer can easily implement. We used CCDSoft software program to control our ccd camera and changing filters whenever required during our observation. We have made use of red, blue, and green filters.

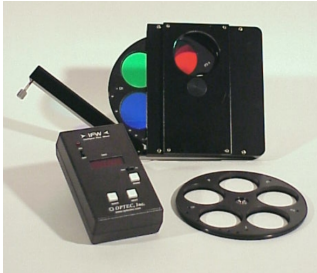

Figure 5: Model IFW Intelligent Filter Wheel

3. Observations

A series of observations took place on 3 different days in the observatory at the Department of Physics and Astrophysics, University of Delhi. They are as follows:

Frames	**Bias**	**Dark**	**Flat**
Date of Observation	29 February 2024	29 February 2024	11 March 2024
Observation Time	8:37 PM	8:38 PM	6:43 PM - 6:56 PM
Total No. of Frames captured	10	10	(5 × 6) in Red, Green, Blue and Open filter each
Exposure time (sec)	0.0	0.001	0.01, 0.02, 0.05, 0.1, 0.2, 0.5

Table 1: Observations of Bias, Dark and Flat

Object	Pleiades (Open Cluster)
Date of Observation	12 March 2024
Observation Period	1hr 05min
Starting time	7:18 PM
Ending time	8:23 PM
Total No. of pictures captured	348
No. of pictures captured per filter	87
Exposure time for Open filter	0.1 sec
Exposure time for Red, Green and Blue filters	0.5 sec

Table 2: Observations for Pleiades

The log entries of the same is available with this report. (see Appendix D)

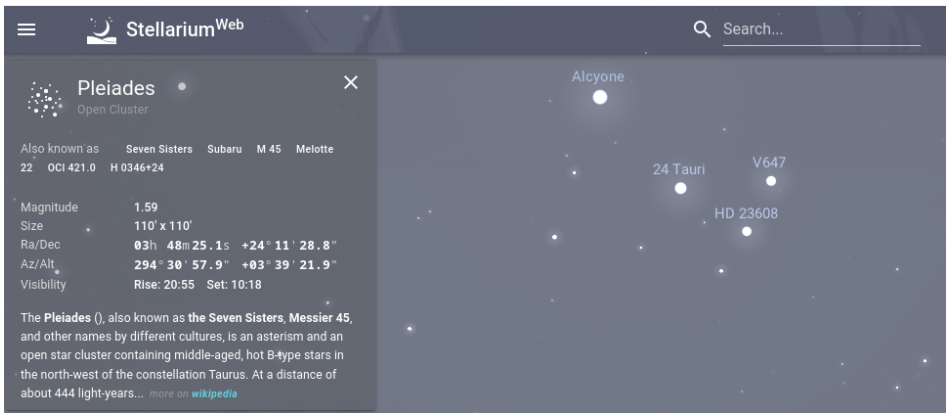

Figure 6: The four stars of Pleiades under observation

4. Data Analysis

4.1. CCD Characterization

4.1.1. Imaging and Calibration:

Along with exposures of the object (light frames), one needs to take bias, dark and flat-field frames to calibrate the light frames, that is, to remove noises and effects of other imperfections in the optical setups.

Light frames: These are the actual exposure images of the objects under observation. These are the raw images to be calibrated using the other bias, dark, and flat-field frames.

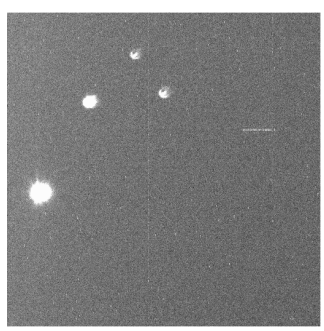

Figure 7: Light Frame (Exposure Time: 0.1 sec , Open Filter)

Bias frames: These are also known as zero exposure frames as they are taken with zero exposure time and with a camera's shutter closed. The purpose of these frames is to subtract the inherent electronic noise of the camera's sensor and readout electronics.

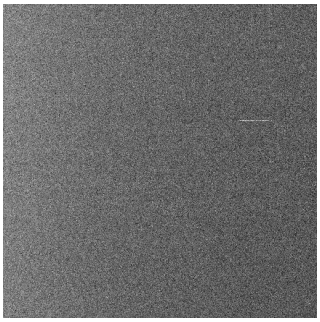

Figure 8: Bias Frame (Exposure Time: 0.00 sec)

Dark frames: These are also taken with a camera's shutter closed but with a non-zero exposure time. These are also known as thermal count images, as the purpose of these frames is to subtract the contribution from thermally generated charge in the image that is accumulated due to long interactions at moderate cooling.

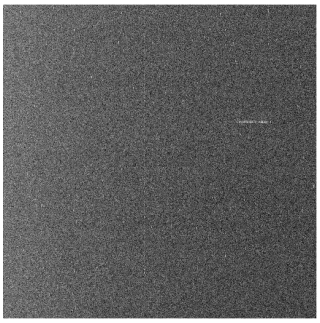

Figure 9: Dark Frame (exposure time: 0.001 sec)

Flat-field frames: Flat fielding corresponds to correcting the combined optical system and CCD throughput at each pixel so that each pixel on the CCD would respond equally to a source with the same photon flux. The purpose of Flat fielding is to remove the effect of the pixel-to-pixel sensitivity variations across the array as well as the effect of dust or scratches on the CCD window. Performing using dome flats or sky flats.

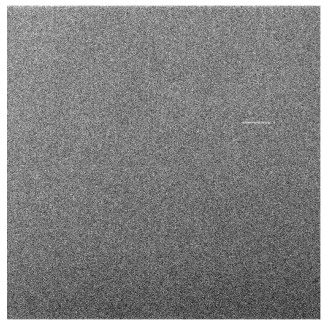

Figure 10: Flat frame (exposure time: 0.5 sec, open filter)

4.1.2. Calculating Gain and Readout Noise:

Using two bias frames and two equal flat-field images, designated 1 and 2, we can proceed as follows. Determine the mean pixel value within each image, say, the mean values of the two bias frames B1 and B2 and likewise F1 and F2 will be the corresponding values for the two flats. Next, create two difference images $(B1 - B2)$ and $(F1 - F2)$ and measure the standard deviation of these image differences: $(B1 - B2)$ and $(F1 - F2)$. Having done that, the gain of the CCD can be determined from the following expression:

$$\text{Gain} = \frac{(\overline{F1} + \overline{F2}) - (\overline{B1} + \overline{B2})}{\sigma^2_{F1-F2} - \sigma^2_{B1-B2}} \tag{4.1}$$

The readout noise can be obtained from

$$\text{Readout noise} = \frac{\text{Gain} \cdot \sigma_{B1-B2}}{\sqrt{2}} \tag{4.2}$$

The arithmetic operations have been carried out in IRAF using *imarith*. For a set of five flats and five biases, a total of 10 possible pairs were generated. Thus, we have 10 data points per exposure time for a particular filter. A total of 60 data points were obtained for a particular filter. This is then plotted to obtain the gain (slope) and hence the read-out noise.

Figure 11: Using imarith and imstat in IRAF

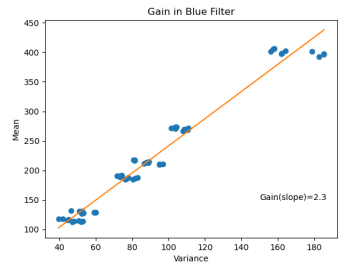

(a) Gain in open filter

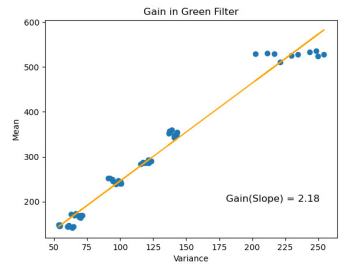

(b) Gain in green filter

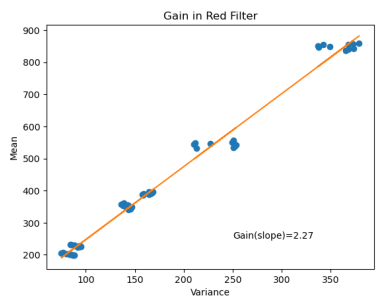

(c) Gain in red filter

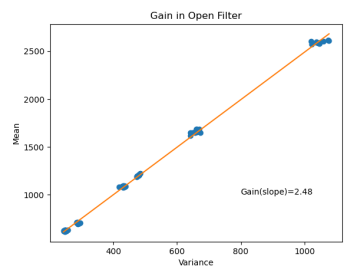

(d) Gain in blue filter

Figure 12: Gain in different filters

mean(fplus)	mean (bplus)	numerator	std(fminus)	std(bminus)	var(fminus)	var(bminus)	denominator	readnoise
2836	224.7	2611.3	33.92	8.573	1150.5664	73.496329	1077.070071	15.03382556
2838	222.3	2615.7	34.01	9.039	1156.6801	81.703521	1074.976579	15.85101472
2827	224.4	2602.6	33.67	8.568	1133.6689	73.410624	1060.258276	15.02505743
2818	225.7	2592.3	33.51	8.583	1122.9201	73.667889	1049.252211	15.05136181
2805	226	2579	33.47	8.54	1120.2409	72.9316	1047.3093	14.97595594
2808	223.6	2584.4	33.53	8.969	1124.2609	80.442961	1043.817939	15.72826099
2817	222.3	2594.7	33.45	8.977	1118.9025	80.586529	1038.315971	15.74228999
							Average:	15.31458089

Figure 13: Table of various expressions calculated for determining gain (open filter). Other tables are available in Appendix A

4.2. Image reduction

In astronomy, image reduction refers to the process of transforming raw telescope data into usable scientific measurements. IRAF (Image Reduction and Analysis Facility) is a powerful software package specifically designed for this purpose. It tackles various tasks involved in reducing astronomical images, especially those captured with CCD detectors. IRAF allows astronomers to perform actions like bias subtraction (removing electronic offsets), flat-field correction (correcting for pixel sensitivity variations), cosmic ray removal (eliminating high-energy particle hits), and image stacking (combining multiple exposures for improved signal-to-noise). Through these steps, IRAF helps transform raw data into cleaner, calibrated images ready for further analysis, such as measuring object brightnesses, positions, or even extracting spectral information.

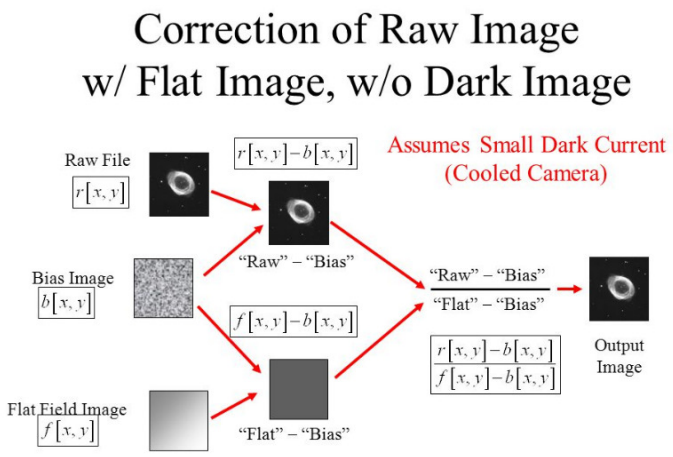

Figure 14: An illustration of image reduction procedure using IRAF.

Bias Reduction:

The first step is to remove the offset level using bias frames. Using *zerocombine* task of *noao>imred>ccdred* to combine the bias frames into a single frame, called the *masterbias.fits* frame. Once this is done, we subtract this *masterbias.fits* from all the other frames (flat-fielded frames and light frames) using the *imarith* task. We don't use dark frames in our analysis because our CCD has cooling system, thus the dark current contribution is negligible.

Flat-Field Reduction: Next, we use *flatcombine* task to make a single *masterflat.fits* which is to be divided from the light frame since flat-fielding is a multiplicative effect. We use *imarith* again

to do the arithmetic operation.

Final Reduction: Finally, we need our light frames free of bias and flat-field. To do this, we use *ccdproc* task of *noao>imred>ccdred* where we give a list of our light frames as a *.list* file, along with our *masterbias.fits* and *masterflat.fits*. Thus we get our final reduced light frames.

4.3. Aperture Photometry of Pleiades Cluster

Photometry is a technique used in astronomy to find the flux radiated by a luminous object. Astronomers, in general, use two types of photometry: aperture photometry and PSF photometry. The former is preferred when there are only a few stars in the observer's field. If the field is crowded, PSF photometry is chosen. Since our field only has four stars, we proceed with aperture photometry.

The basic principle of aperture photometry is as follows: enclose the star in a circular aperture of some radius r, add all the light in that circle and subtract off the amount of light contributed by the sky background in that same area. The result is the brightness of the star. The advantage of aperture photometry is that it gives an absolute measurement, in the sense that it provides the number of photoelectrons generated by the star in a particular exposure time.

IRAF comes with predefined packages to perform aperture photometry. We use *apphot* to perform photometry on the four stars of Pleiades cluster that is in the field - Alcyone, 24 Tauri, v647 Tauri and HD 23608.

Once the light frames are bias and flat-field corrected, the next step is to use *apphot*. Before directly performing photometry on a particular frame, the following parameters are to be modified accordingly:

- datapars
- centerpars
- fitskypars
- photpars

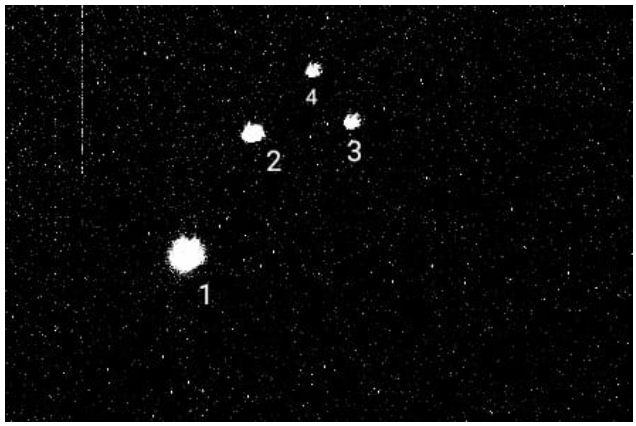

Figure 15: The sequence of stars considered during the observation.

Note: The distribution of the star on the CCD is of a Gaussian shape. So, one should have the information of the FWHM of each star and the standard deviation of the background before starting aperture photometry. These information can be obtained using the interactive mode of DS9. Open the required light frame using *imexamine* function and press *A* having the cursor on each star in the sequence mentioned in 15. As a result, the generated log file would have the required values.

datapars: This functionality helps us edit the parameters required to specify the FWHM of a particular star in the frame and the standard deviation of the background. The readout noise and gain of that particular frame should also be entered.

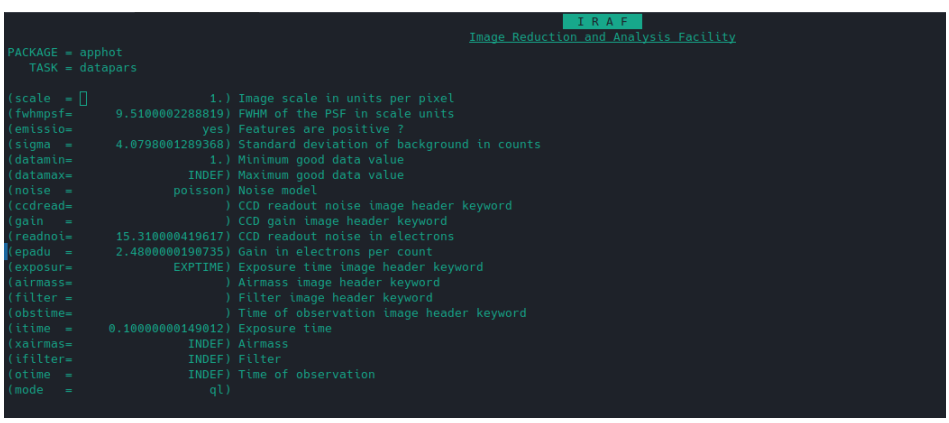

```
                                                                    I R A F
                                                        Image Reduction and Analysis Facility
PACKAGE = apphot
   TASK = datapars

(scale  =                  1.) Image scale in units per pixel
(fwhmpsf=       9.5100002288819) FWHM of the PSF in scale units
(emissio=                  yes) Features are positive ?
(sigma  =       4.0798001289368) Standard deviation of background in counts
(datamin=                   1.) Minimum good data value
(datamax=                INDEF) Maximum good data value
(noise  =               poisson) Noise model
(ccdread=                      ) CCD readout noise image header keyword
(gain   =                      ) CCD gain image header keyword
(readnoi=       15.310000419617) CCD readout noise in electrons
(epadu  =       2.4800000190735) Gain in electrons per count
(exposur=               EXPTIME) Exposure time image header keyword
(airmass=                      ) Airmass image header keyword
(filter =                      ) Filter image header keyword
(obstime=                      ) Time of observation image header keyword
(itime  =      0.10000000149012) Exposure time
(xairmas=                INDEF) Airmass
(ifilter=                INDEF) Filter
(otime  =                INDEF) Time of observation
(mode   =                   ql)
```

Figure 16: List of datapar parameters whose values are to be set according to our star in observation

centerpars: These parameters are used to redetermine each object's (x,y) coordinates based on some weighting scheme given by "calgorithm". The value of cbox can be anything around 1-2 × FWHM to include sufficient pixels for centering but not so large as to include a lot of noise. Here we have taken cbox to be 1.5 × FWHM.

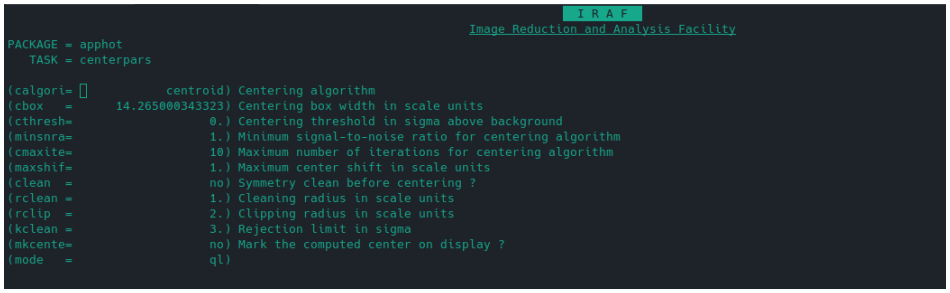

Figure 17: List of centerpars parameters whose values are to be set according to our star in observation

fitskypars: These parameters define the annular region around each star that will be used to measure the local sky brightness. The following are the values that we have used in our analysis. Note that the annulus is fourfold of the FWHM of the star while the dannulus is half the annulus. This forms a ring of radius 4 × FWHM and of thickness 0.5 × annulus.

Figure 18: List of fitskypars parameters whose values are to be set according to our star in observation

photpars: This set of parameters takes a list of aperture radii and calculates the magnitude within that particular aperture radius. As a result, we get a list of apertures along with the calculated instrumental magnitudes. The parameters are as follows. Note that the aperture radii are taken starting from FWHM and ends at 5 × FWHM with an increment of 0.1 units. Once the *phot* command is executed with the input file, we obtain a *.mag* file that consists of a series of radius

and their corresponding magnitudes.

```
PACKAGE = apphot
   TASK = photpars

(weighti= []           constant) Photometric weighting scheme for wphot
(apertur=       9.51:57.06:0.1) List of aperture radii in scale units
(zmag   =                  25.) Zero point of magnitude scale
(mkapert=                   no) Draw apertures on the display
(mode   =                   ql)
```

Figure 19: List of photpars parameters whose values are to be set according to our star in observation

Curve of Growth: To determine the final absolute magnitude, we plot the magnitudes versus different aperture radii. This is called "curve of growth". We take only the radius and magnitude, make a curve of growth and observe where this curve becomes constant. The value of magnitude at this region is the absolute instrumental magnitude of the star.

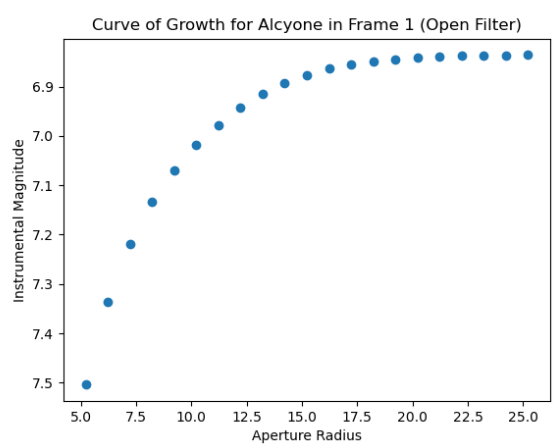

Figure 20: Curve of growth obtained for Alcyone in open filter. The instrumental magnitude turns out to be 6.84

4.4. Extinction Coefficients

Extinction coefficient is a necessary quantity to be determined while calculating the absolute magnitude of a star. Let us see how to find the extinction coefficient considering a few necessary factors:

4.4.1. Airmass

Airmass is the quantity of atmosphere present in the line of sight of the observer and the source. This can be measured from the zenith angle of the source as follows:

$$\chi = sec(z) \tag{4.3}$$

where χ is the airmass and z is the zenith angle of the source.

This can be determined using the cosine rule:

$$sec(z) = \frac{1}{cos(\phi_0)cos(\delta) + sin(\phi_0)sin(\delta)cos(h)} \tag{4.4}$$

where ϕ_0 is the observer's latitude, δ is the declination of the source and h is the hour angle of the source.

Hour angle can be determined by using

$$HourAngle(HA) = LocalSiderialTime(LST) - RightAscension(RA) \tag{4.5}$$

4.4.2. Local Siderial Time (LST)

The header of a fits file usually has details like date and time of observation ('DATE-OBS' and 'TIME-OBS' keywords). But the time is not typically in LST, but in UTC. So, what we do first is to find the Greenwich Siderial Time (GST) from UTC and then convert it to LST with the information available on the observer's latitude.

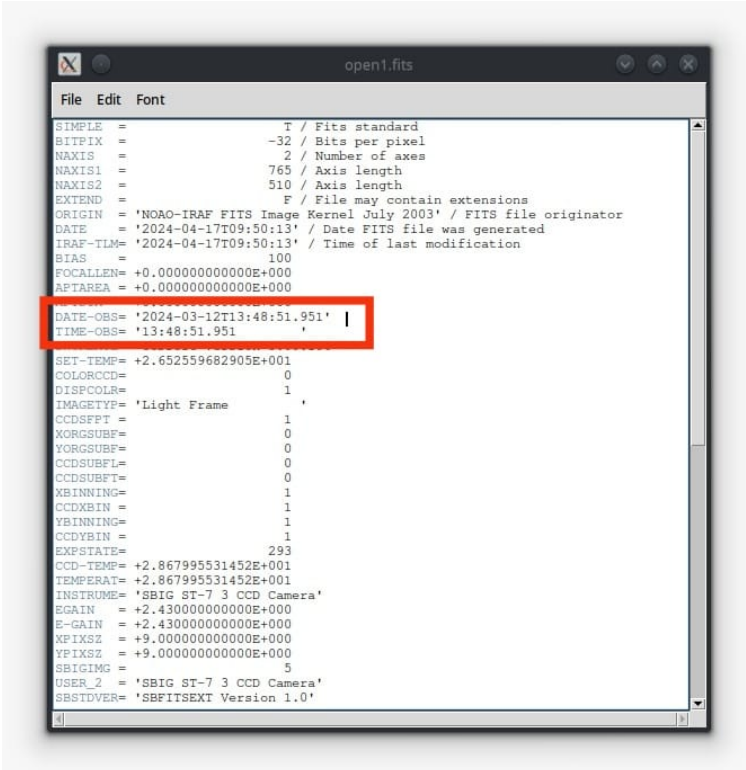

Figure 21: Header file of a frame from open filter. Note that there are two keywords 'DATE-OBS' and 'TIME-OBS' which contains the UTC date and time of the frame.

The conversion of UTC to GST is given by

$$GST = G + 0.0657098244 \times d + 1.00273791 \times t \tag{4.6}$$

where G is the GST at 0^h on December 31st (previous year), d is the day number during the year and t is the UTC time.

4.4.3. Calculation of LST and Airmass in Python

We have predefined modules in Python to carry out the above mentioned conversion. The following code snippet shows how the conversion and hence the determination of airmass is done.

Listing 1: Code snippet for calculating the airmass

```
from astropy.coordinates import SkyCoord, AltAz
from astropy.time import Time
from astropy.io import fits
```

```
from astropy.coordinates import EarthLocation, AltAz, SkyCoord
import astropy.units as u
import os
files = os.listdir('/home/luciferat022/Desktop/Open_Analysis')


# Define the location of Department of Physics and Astrophysics, University of Delhi
dopa = EarthLocation(lat=28.6887*u.deg, lon=77.2118*u.deg, height=250*u.m)

# List of names of stars under observation
stars=['Alcyone','24 tauri','v647 tauri', 'hd 23608']

for star in stars:
    print(star)
    # Extract the RA and DEC of the star
    star = SkyCoord.from_name(star)

    for _file in files:
        with fits.open(os.path.join('/home/Desktop/Open_Analysis', _file)) as hdulist:

            # Loop through each HDU in the FITS file
            for idx, hdu in enumerate(hdulist):
                index=_file.split('.')
                s=hdu.header['DATE-OBS']

                # Define the time (extracts the time of observation from header)
                time = Time(s)

                # Calculate the altitude and azimuth of the star at the given time and location
                star_altaz = star.transform_to(AltAz(obstime=time, location=dopa))

                # Get the airmass at the obtained zenith angle
                airmass = star_altaz.secz

                print("Airmass for the Alcyone at LST 6h22m49.53006944s for dopa is:", airmass)
```

Hence, we get the airmass for each frame under consideration.

4.4.4. Extinction coefficient

Extinction coefficient is related to the absorption and emission of photons by the earth's atmosphere or the interstellar gas and dust. To determine the true magnitude of a star, one should take the

extinction coefficients into consideration. While interstellar extinction is mostly rectified when dealing with distant objects such as stars, galaxies and quasars, we have only rectified for the atmospheric extinction.

$$m_{instrumental} = m_{calibrated} + K\chi \tag{4.7}$$

where K is the extinction coefficient and χ is the airmass. Thus one could get the extinction coefficient from the slope of the graph of instrumental magnitude, $m_{instrumental}$, plotted against the airmass. The intercept gives the calibrated magnitude, $m_{calibrated}$, of the star. The following graphs show the extinction coefficients of star 1 and star 2 in different filters. See Appendix B for the extinction coefficients of the other two stars.

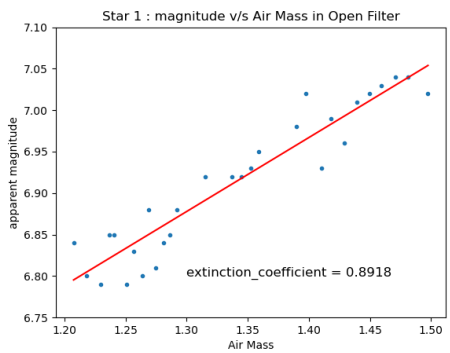

(a) Extinction coefficient in open filter

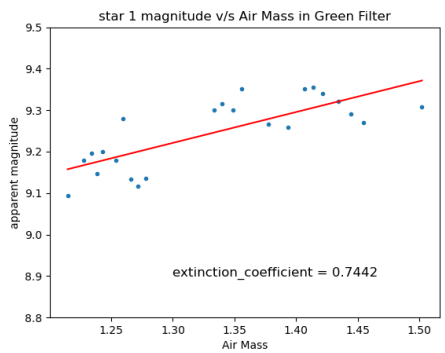

(b) Extinction coefficient in green filter

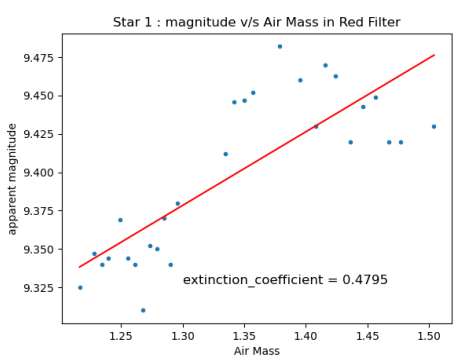

(c) Extinction coefficient in red filter

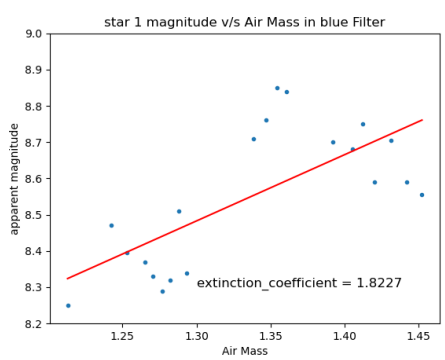

(d) Extinction coefficient in blue filter

Figure 22: Extinction coefficient in different filters for star 1

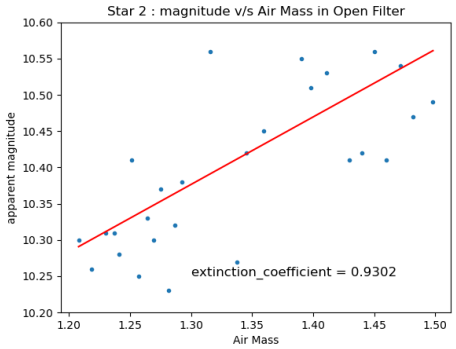

(a) Extinction coefficient in open filter

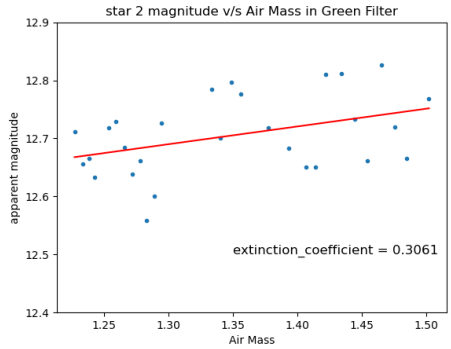

(b) Extinction coefficient in green filter

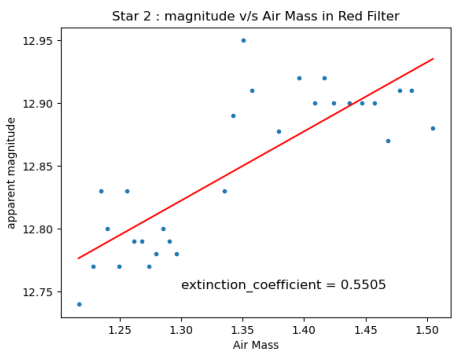

(c) Extinction coefficient in red filter

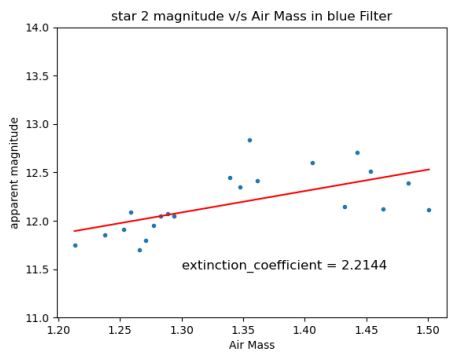

(d) Extinction coefficient in blue filter

Figure 23: Extinction coefficient in different filters for star 2

5. Result and Conclusion

5.1. Result

The readout noise and gain of CCD in different filters are found to be:

Filters	**Readout noise** (electrons/pixel)	**Gain** (electrons/ADU)
open	15.31	2.48
green	15.16	2.18
red	14.01	2.27
blue	14.19	2.30

Table 3: Readout noise and gain

The instrumental magnitude and extinction coefficients for star 1 in different filters are found to be:

Filters	**Extinction Coefficient**	**Instrumental Magnitude**
open	0.8918	5.7185 ± 0.001
green	0.7442	8.2536 ± 0.001
red	0.4795	8.754 ± 0.001
blue	1.8227	6.1132 ± 0.001

Table 4: STAR 1 : Alcyone

The instrumental magnitude and extinction coefficients for star 2 in different filters are found to be:

Filters	**Extinction Coefficient**	**Instrumental Magnitude**
open	0.9302	9.1672 ± 0.004
green	0.3061	12.291 ± 0.006
red	0.5505	12.106 ± 0.006
blue	2.2144	9.207 ± 0.007

Table 5: STAR 2 : 24 TAURI

5.2. Conclusion

- From Table 3, we conclude that the CCD characteristics - **readout noise** is approximately equal to 15 electrons/pixel while **gain** is approximately equal 2.5 electrons/ADU.
- We find the calibrated magnitude which gives the apparent magnitude of the star under study. The slope of the apparant magnitude vs airmass plot (Figure 23) of a star gives us the extinction coefficient which provides information about the amount of attenuation or dimming of light.
- Our investigation reveals a linear relationship between instrumental magnitude and air mass. As airmass increases, instrumental magnitude also increases, indicating a progressive dimming of the observed stars. This trend aligns with our expectations based on atmospheric effects.
- We have observed that the calibrated magnitude of different stars is lower in the blue filter compared to the red and green filters (Table 4 and Table 5). This observation suggests that the observed stars emit a substantial amount of light in the blue portion of the spectrum. This finding enhances our understanding of the spectral characteristics of the stars studied.

Appendices

A Readout Noise and Gain Tables

There are 5 bias frames and 5 flat fields (per exposure time) in total. We can generate 10 pairs per filter per exposure time as follows:

$$^{5}C_{2} = 10 \tag{A-1}$$

Frame 1	**Frame2**
flat1.fits	flat2.fits
flat1.fits	flat3.fits
flat1.fits	flat4.fits
flat1.fits	flat5.fits
flat2.fits	flat3.fits
flat2.fits	flat4.fits
flat2.fits	flat5.fits
flat3.fits	flat4.fits
flat3.fits	flat5.fits
flat4.fits	flat5.fits

Table 6: Here is an example of the selection of pairs

Since we have flat-fields in 6 different exposure times, we obtain a total of 60 data points.

$\bar{F_1} + \bar{F_2}$	$\bar{B_1} + \bar{B_2}$	$(\bar{F_1} + \bar{F_2}) - (\bar{B_1} + \bar{B_2})$	$\sigma_{F_1-F_2}$	$\sigma_{B_1-B_2}$	$\sigma^2_{F_1-F_2}$	$\sigma^2_{B_1-B_2}$	$\sigma^2_{F_1-F_2} - \sigma^2_{B_1-B_2}$	**Readout Noise**
2836	224.7	2611.3	33.92	8.573	1150.5664	73.496329	1077.070071	15.03382556
2838	222.3	2615.7	34.01	9.039	1156.6801	81.703521	1074.976579	15.85101472
2827	224.4	2602.6	33.67	8.568	1133.6689	73.410624	1060.258276	15.02505743
2818	225.7	2592.3	33.51	8.583	1122.9201	73.667889	1049.252211	15.05136181
2805	226	2579	33.47	8.54	1120.2409	72.9316	1047.3093	14.97595594
2808	223.6	2584.4	33.53	8.969	1124.2609	80.442961	1043.817939	15.72826099
2817	222.3	2594.7	33.45	8.977	1118.9025	80.586529	1038.315971	15.74228999
2814	224.7	2589.3	33.33	8.54	1110.8889	72.9316	1037.9573	14.97595594
2797	225.7	2571.3	33.1	8.542	1095.61	72.965764	1022.644236	14.97946319
2826	222.6	2603.4	33.2	9	1102.24	81	1021.24	15.78262336
1875	224.4	1650.6	27.32	8.568	746.3824	73.410624	672.971776	15.02505743
1911	224.7	1686.3	27.26	8.573	743.1076	73.496329	669.611271	15.03382556

1906	222.3	1683.7	27.27	9.039	743.6529	81.703521	661.949379	15.85101472
1877	224.7	1652.3	27.1	8.54	734.41	72.9316	661.4784	14.97595594
1908	222.6	1685.4	27.21	9	740.3841	81	659.3841	15.78262336
1877	225.7	1651.3	27.02	8.583	730.0804	73.667889	656.412511	15.05136181
1879	226	1653	26.96	8.54	726.8416	72.9316	653.91	14.97595594
1872	222.3	1649.7	26.97	8.977	727.3809	80.586529	646.794371	15.74228999
1875	223.6	1651.4	26.87	8.969	721.9969	80.442961	641.553939	15.72826099
1844	225.7	1618.3	26.73	8.542	714.4929	72.965764	641.527136	14.97946319
1445	222.6	1222.4	23.77	9	565.0129	81	484.0129	15.78262336
1439	222.3	1216.7	23.75	9.039	564.0625	81.703521	482.358979	15.85101472
1432	224.7	1207.3	23.54	8.54	554.1316	72.9316	481.2	14.97595594
1436	224.7	1211.3	23.55	8.573	554.6025	73.496329	481.106171	15.03382556
1436	222.3	1213.7	23.68	8.977	560.7424	80.586529	480.155871	15.74228999
1429	223.6	1205.4	23.66	8.969	559.7956	80.442961	479.352639	15.72826099
1425	226	1199	23.49	8.54	551.7801	72.9316	478.8485	14.97595594
1426	224.4	1201.6	23.43	8.568	548.9649	73.410624	475.554276	15.02505743
1420	225.7	1194.3	23.39	8.583	547.0921	73.667889	473.424211	15.05136181
1416	225.7	1190.3	23.36	8.542	545.6896	72.965764	472.723836	14.97946319
1315	226	1089	22.61	8.54	511.2121	72.9316	438.2805	14.97595594
1309	224.7	1084.3	22.54	8.54	508.0516	72.9316	435.12	14.97595594
1311	225.7	1085.3	22.54	8.583	508.0516	73.667889	434.383711	15.05136181
1320	224.7	1095.3	22.53	8.573	507.6009	73.496329	434.104571	15.03382556
1305	224.4	1080.6	22.52	8.568	507.1504	73.410624	433.739776	15.02505743
1319	222.6	1096.4	22.62	9	511.6644	81	430.6644	15.78262336
1301	225.7	1075.3	22.43	8.542	503.1049	72.965764	430.139136	14.97946319
1315	222.3	1092.7	22.62	9.039	511.6644	81.703521	429.960879	15.85101472
1311	223.6	1087.4	22.51	8.969	506.7001	80.442961	426.257139	15.72826099
1304	222.3	1081.7	22.33	8.977	498.6289	80.586529	418.042371	15.74228999
933.9	224.7	709.2	19.22	8.573	369.4084	73.496329	295.912071	15.03382556
925	226	699	19.11	8.54	365.1921	72.9316	292.2605	14.97595594
929.5	224.4	705.1	19.12	8.568	365.5744	73.410624	292.163776	15.02505743
931	224.7	706.3	19.06	8.54	363.2836	72.9316	290.352	14.97595594
923.6	225.7	697.9	19.04	8.583	362.5216	73.667889	288.853711	15.05136181
920.7	225.7	695	19.01	8.542	361.3801	72.965764	288.414336	14.97946319
936.9	222.3	714.6	19.22	9.039	369.4084	81.703521	287.704879	15.85101472
938.3	222.6	715.7	19.16	9	367.1056	81	286.1056	15.78262336
928	223.6	704.4	19.11	8.969	365.1921	80.442961	284.749139	15.72826099
934	222.3	711.7	19.1	8.977	364.81	80.586529	284.223471	15.74228999
858	224.7	633.3	18.18	8.573	330.5124	73.496329	257.016071	15.03382556
849.1	224.4	624.7	18.1	8.568	327.61	73.410624	254.199376	15.02505743
849.3	224.7	624.6	18.05	8.54	325.8025	72.9316	252.8709	14.97595594
846.9	226	620.9	18.03	8.54	325.0809	72.9316	252.1493	14.97595594
846.7	225.7	621	18.01	8.583	324.3601	73.667889	250.692211	15.05136181
855.2	222.6	632.6	18.18	9	330.5124	81	249.5124	15.78262336
855	222.3	632.7	18.16	9.039	329.7856	81.703521	248.082079	15.85101472
838	225.7	612.3	17.9	8.542	320.41	72.965764	247.444236	14.97946319
846.3	222.3	624	18.02	8.977	324.7204	80.586529	244.133871	15.74228999
843.9	223.6	620.3	17.99	8.969	323.6401	80.442961	243.197139	15.72826099
							Average:	15.31458089

Table 7: Readout noise for open filter

$\bar{F_1} + \bar{F_2}$	$\bar{B_1} + \bar{B_2}$	$(\bar{F_1} + \bar{F_2}) - (\bar{B_1} + \bar{B_2})$	$\sigma_{F_1-F_2}$	$\sigma_{B_1-B_2}$	$\sigma^2_{F_1-F_2}$	$\sigma^2_{B_1-B_2}$	$\sigma^2_{F_1-F_2} - \sigma^2_{B_1-B_2}$	**Readout Noise**
1082	-222.6	859.4	21.45	9	460.1025	-81	379.1025	14.4461915396412

1077	-222.3	854.7	20.6	9.039	424.36	-81.703521	342.656479	14.5087917029796
1073	-222.3	850.7	20.44	8.977	417.7936	-80.586529	337.207071	14.4092734945954
1067	-223.6	843.4	21.3	8.969	453.69	-80.442961	373.247039	14.3964324354491
1082	-224.7	857.3	21.12	8.573	446.0544	-73.496329	372.558071	13.7608000077049
1079	-224.7	854.3	21	8.54	441	-72.9316	368.0684	13.7078306387262
1072	-226	846	20.27	8.54	410.8729	-72.9316	337.9413	13.7078306387262
1073	-224.4	848.6	20.55	8.568	422.3025	-73.410624	348.891876	13.7527743457384
1067	-225.7	841.3	21.02	8.583	441.8404	-73.667889	368.172511	13.7768513316378
1063	-225.7	837.3	20.93	8.542	438.0649	-72.965764	365.099136	13.7110409035128
778.6	-222.6	556	18.22	9	331.9684	-81	250.9684	14.4461915396412
773.5	-222.3	551.2	18.19	9.039	330.8761	-81.703521	249.172579	14.5087917029796
770.6	-222.3	548.3	17.09	8.977	292.0681	-80.586529	211.481571	14.4092734945954
768.5	-223.6	544.9	17.06	8.969	291.0436	-80.442961	210.600639	14.3964324354491
770.8	-224.7	546.1	17.34	8.573	300.6756	-73.496329	227.179271	13.7608000077049
767.8	-224.7	543.1	18.06	8.54	326.1636	-72.9316	253.232	13.7078306387262
765.7	-226	539.7	18.03	8.54	325.0809	-72.9316	252.1493	13.7078306387262
762.7	-224.4	538.3	18.05	8.568	325.8025	-73.410624	252.391876	13.7527743457384
760.7	-225.7	535	18.02	8.583	324.7204	-73.667889	251.052511	13.7768513316378
757.7	-225.7	532	16.9	8.542	285.61	-72.965764	212.644236	13.7110409035128
584.2	-222.6	361.6	14.83	9	219.9289	-81	138.9289	14.4461915396412
578.9	-222.3	356.6	14.75	9.039	217.5625	-81.703521	135.858979	14.5087917029796
576.2	-222.3	353.9	14.79	8.977	218.7441	-80.586529	138.157571	14.4092734945954
574.3	-223.6	350.7	14.91	8.969	222.3081	-80.442961	141.865139	14.3964324354491
579.2	-224.7	354.5	14.71	8.573	216.3841	-73.496329	142.887771	13.7608000077049
576.4	-224.7	351.7	14.72	8.54	216.6784	-72.9316	143.7468	13.7078306387262
574.6	-226	348.6	14.82	8.54	219.6324	-72.9316	146.7008	13.7078306387262
571.2	-224.4	346.8	14.67	8.568	215.2089	-73.410624	141.798276	13.7527743457384
569.3	-225.7	343.6	14.8	8.583	219.04	-73.667889	145.372111	13.7768513316378
566.6	-225.7	340.9	14.72	8.542	216.6784	-72.965764	143.712636	13.7110409035128
428.7	-222.6	206.1	12.56	9	157.7536	-81	76.7536	14.4461915396412
427.9	-222.3	205.6	12.52	9.039	156.7504	-81.703521	75.046879	14.5087917029796
427.2	-222.3	204.9	12.55	8.977	157.5025	-80.586529	76.915971	14.4092734945954
426.2	-223.6	202.6	12.66	8.969	160.2756	-80.442961	79.832639	14.3964324354491
427	-224.7	202.3	12.5	8.573	156.25	-73.496329	82.753671	13.7608000077049
426.3	-224.7	201.6	12.57	8.54	158.0049	-72.9316	85.0733	13.7078306387262
425.3	-226	199.3	12.69	8.54	161.0361	-72.9316	88.1045	13.7078306387262
425.5	-224.4	201.1	12.54	8.568	157.2516	-73.410624	83.840976	13.7527743457384
424.5	-225.7	198.8	12.68	8.583	160.7824	-73.667889	87.114511	13.7768513316378
423.8	-225.7	198.1	12.65	8.542	160.0225	-72.965764	87.056736	13.7110409035128
454.6	-222.6	232	12.89	9	166.1521	-81	85.1521	14.4461915396412
454	-222.3	231.7	12.87	9.039	165.6369	-81.703521	83.933379	14.5087917029796
452.9	-222.3	230.6	12.99	8.977	168.7401	-80.586529	88.153571	14.4092734945954
452.4	-223.6	228.8	12.99	8.969	168.7401	-80.442961	88.297139	14.3964324354491
452.6	-224.7	227.9	12.89	8.573	166.1521	-73.496329	92.655771	13.7608000077049
451.5	-224.7	226.8	12.94	8.54	167.4436	-72.9316	94.512	13.7078306387262
451	-226	225	12.93	8.54	167.1849	-72.9316	94.2533	13.7078306387262
450.9	-224.4	226.5	12.97	8.568	168.2209	-73.410624	94.810276	13.7527743457384
450.4	-225.7	224.7	12.94	8.583	167.4436	-73.667889	93.775711	13.7768513316378
449.3	-225.7	223.6	12.82	8.542	164.3524	-72.965764	91.386636	13.7110409035128
619.4	-222.6	396.8	15.66	9	245.2356	-81	164.2356	14.4461915396412
618.7	-222.3	396.4	15.82	9.039	250.2724	-81.703521	168.568879	14.5087917029796
617.5	-222.3	395.2	15.77	8.977	248.6929	-80.586529	168.106371	14.4092734945954
615.6	-223.6	392	15.74	8.969	247.7476	-80.442961	167.304639	14.3964324354491
617	-224.7	392.3	15.46	8.573	239.0116	-73.496329	165.515271	13.7608000077049
615.8	-224.7	391.1	15.45	8.54	238.7025	-72.9316	165.7709	13.7078306387262
613.9	-226	387.9	15.4	8.54	237.16	-72.9316	164.2284	13.7078306387262

615.1	-224.4	390.7	15.25	8.568	232.5625	-73.410624	159.151876	13.7527743457384
613.2	-225.7	387.5	15.21	8.583	231.3441	-73.667889	157.676211	13.7768513316378
612	-225.7	386.3	15.21	8.542	231.3441	-72.965764	158.378336	13.7110409035128
							Average =	14.0177817038712

Table 8: Readout noise for red filter

$\bar{F_1} + \bar{F_2}$	$\bar{B_1} + \bar{B_2}$	$(\bar{F_1} + \bar{F_2}) - (\bar{B_1} + \bar{B_2})$	$\sigma_{F_1-F_2}$	$\sigma_{B_1-B_2}$	$\sigma^2_{F_1-F_2}$	$\sigma^2_{B_1-B_2}$	$\sigma^2_{F_1-F_2} - \sigma^2_{B_1-B_2}$	**Readout Noise**
758.7	222.6	536.1	18.15	9	329.4225	81	248.4225	13.8734350468801
755.4	222.3	533.1	18.03	9.039	325.0809	81.703521	243.377379	13.9335532654165
751.5	222.3	529.2	16.82	8.977	282.9124	80.586529	202.325871	13.8379807128714
753.5	223.6	529.9	17.24	8.969	297.2176	80.442961	216.774639	13.8256487706075
755.9	224.7	531.2	16.87	8.573	284.5969	73.496329	211.100571	13.2152176285448
752	224.7	527.3	18.09	8.54	327.2481	72.9316	254.3165	13.1643483667062
754	226	528	17.53	8.54	307.3009	72.9316	234.3693	13.1643483667062
748.6	224.4	524.2	17.97	8.568	322.9209	73.410624	249.510276	13.2075101646298
750.7	225.7	525	17.42	8.583	303.4564	73.667889	229.788511	13.2306325563746
736.8	225.7	511.1	17.15	8.542	294.1225	72.965764	221.156736	13.1674313522722
582.6	222.6	360	14.84	9	220.2256	81	139.2256	13.8734350468801
579.3	222.3	357	14.8	9.039	219.04	81.703521	137.336479	13.9335532654165
576.8	222.3	354.5	14.77	8.977	218.1529	80.586529	137.566371	13.8379807128714
575	223.6	351.4	14.74	8.969	217.2676	80.442961	136.824639	13.8256487706075
578.9	224.7	354.2	14.72	8.573	216.6784	73.496329	143.182071	13.2152176285448
576.4	224.7	351.7	14.69	8.54	215.7961	72.9316	142.8645	13.1643483667062
574.6	226	348.6	14.69	8.54	215.7961	72.9316	142.8645	13.1643483667062
573.1	224.4	348.7	14.65	8.568	214.6225	73.410624	141.211876	13.2075101646298
571.3	225.7	345.6	14.65	8.583	214.6225	73.667889	140.954611	13.2306325563746
568.8	225.7	343.1	14.63	8.542	214.0369	72.965764	141.071136	13.1674313522722
474.8	222.6	252.2	13.17	9	173.4489	81	92.4489	13.8734350468801
474.1	222.3	251.8	13.14	9.039	172.6596	81.703521	90.956079	13.9335532654165
472.2	222.3	249.9	13.21	8.977	174.5041	80.586529	93.917571	13.8379807128714
469.5	223.6	245.9	13.23	8.969	175.0329	80.442961	94.589939	13.8256487706075
471.4	224.7	246.7	13.11	8.573	171.8721	73.496329	98.375771	13.2152176285448
469.5	224.7	244.8	13.16	8.54	173.1856	72.9316	100.254	13.1643483667062
466.8	226	240.8	13.18	8.54	173.7124	72.9316	100.7808	13.1643483667062
468.8	224.4	244.4	13.13	8.568	172.3969	73.410624	98.986276	13.2075101646298
466.1	225.7	240.4	13.17	8.583	173.4489	73.667889	99.781011	13.2306325563746
464.2	225.7	238.5	13.03	8.542	169.7809	72.965764	96.815136	13.1674313522722
371.5	222.6	148.9	11.64	9	135.4896	81	54.4896	13.8734350468801
371.3	222.3	149	11.62	9.039	135.0244	81.703521	53.320879	13.9335532654165
368.6	222.3	146.3	11.61	8.977	134.7921	80.586529	54.205571	13.8379807128714
369	223.6	145.4	11.59	8.969	134.3281	80.442961	53.885139	13.8256487706075
372.2	224.7	147.5	11.61	8.573	134.7921	73.496329	61.295771	13.2152176285448
369.6	224.7	144.9	11.73	8.54	137.5929	72.9316	64.6613	13.1643483667062
370	226	144	11.53	8.54	132.9409	72.9316	60.0093	13.1643483667062
369.4	224.4	145	11.59	8.568	134.3281	73.410624	60.917476	13.2075101646298
369.8	225.7	144.1	11.58	8.583	134.0964	73.667889	60.428511	13.2306325563746
367.1	225.7	141.4	11.7	8.542	136.89	72.965764	63.924236	13.1674313522722
396.1	222.6	173.5	12.14	9	147.3796	81	66.3796	13.8734350468801
394.2	222.3	171.9	12.02	9.039	144.4804	81.703521	62.776879	13.9335532654165
394.7	222.3	172.4	12.11	8.977	146.6521	80.586529	66.065571	13.8379807128714
392.7	223.6	169.1	12.08	8.969	145.9264	80.442961	65.483439	13.8256487706075
394	224.7	169.3	12.04	8.573	144.9616	73.496329	71.465271	13.2152176285448
394.5	224.7	169.8	11.96	8.54	143.0416	72.9316	70.11	13.1643483667062

392.5	226	166.5	11.95	8.54	142.8025	72.9316	69.8709	13.1643483667062
392.6	224.4	168.2	12	8.568	144	73.410624	70.589376	13.2075101646298
390.6	225.7	164.9	11.98	8.583	143.5204	73.667889	69.852511	13.2306325563746
391.1	225.7	165.4	11.92	8.542	142.0864	72.965764	69.120636	13.1674313522722
515.4	222.6	292.8	14.25	9	203.0625	81	122.0625	13.8734350468801
515.1	222.3	292.8	14.24	9.039	202.7776	81.703521	121.074079	13.9335532654165
512.9	222.3	290.6	14.28	8.977	203.9184	80.586529	123.331871	13.8379807128714
514.1	223.6	290.5	14.24	8.969	202.7776	80.442961	122.334639	13.8256487706075
512.7	224.7	288	13.81	8.573	190.7161	73.496329	117.219771	13.2152176285448
510.6	224.7	285.9	13.95	8.54	194.6025	72.9316	121.6709	13.1643483667062
511.7	226	285.7	13.93	8.54	194.0449	72.9316	121.1133	13.1643483667062
510.3	224.4	285.9	13.87	8.568	192.3769	73.410624	118.966276	13.2075101646298
511.4	225.7	285.7	13.84	8.583	191.5456	73.667889	117.877711	13.2306325563746
509.3	225.7	283.6	13.73	8.542	188.5129	72.965764	115.547136	13.1674313522722
							Average =	13.4620106231009

Table 9: Readout noise for green filter

$\bar{F_1} + \bar{F_2}$	$\bar{B_1} + \bar{B_2}$	$(\bar{F_1} + \bar{F_2}) - (\bar{B_1} + \bar{B_2})$	$\sigma_{F_1-F_2}$	$\sigma_{B_1-B_2}$	$\sigma^2_{F_1-F_2}$	$\sigma^2_{B_1-B_2}$	$\sigma^2_{F_1-F_2} - \sigma^2_{B_1-B_2}$	**Readout Noise**
622.4	224.7	397.7	16.09	8.573	258.8881	73.496329	185.391771	13.93659877
621	224.4	396.6	16.08	8.568	258.5664	73.410624	185.155776	13.92847058
618.2	225.7	392.5	16.01	8.583	256.3201	73.667889	182.652211	13.95285516
623.4	222.3	401.1	16.14	9.039	260.4996	81.703521	178.796079	14.69414631
626.9	224.7	402.2	15.4	8.54	237.16	72.9316	164.2284	13.8829527
624	226	398	15.34	8.54	235.3156	72.9316	162.384	13.8829527
622.7	225.7	397	15.33	8.542	235.0089	72.965764	162.043136	13.88620398
629.4	222.6	406.8	15.46	9	239.0116	81	158.0116	14.63074641
628.1	222.3	405.8	15.43	8.977	238.0849	80.586529	157.498371	14.59335672
625.2	223.6	401.6	15.38	8.969	236.5444	80.442961	156.101439	14.58035162
496.5	224.7	271.8	13.56	8.54	183.8736	72.9316	110.942	13.8829527
494.9	226	268.9	13.54	8.54	183.3316	72.9316	110.4	13.8829527
494.8	224.7	270.1	13.52	8.573	182.7904	73.496329	109.294071	13.93659877
494.2	225.7	268.5	13.5	8.542	182.25	72.965764	109.284236	13.88620398
494.1	224.4	269.7	13.49	8.568	181.9801	73.410624	108.569476	13.92847058
492.5	225.7	266.8	13.48	8.583	181.7104	73.667889	108.042511	13.95285516
496.4	222.6	273.8	13.62	9	185.5044	81	104.5044	14.63074641
495.7	222.3	273.4	13.58	8.977	184.4164	80.586529	103.829871	14.59335672
494	223.6	270.4	13.57	8.969	184.1449	80.442961	103.701939	14.58035162
494	222.3	271.7	13.54	9.039	183.3316	81.703521	101.628079	14.69414631
437.1	226	211.1	13.03	8.54	169.7809	72.9316	96.8493	13.8829527
436.2	225.7	210.5	12.99	8.583	168.7401	73.667889	95.072211	13.95285516
435.2	225.7	209.5	12.96	8.542	167.9616	72.965764	94.995836	13.88620398
438.5	223.6	214.9	13.02	8.969	169.5204	80.442961	89.077439	14.58035162
437.3	224.7	212.6	12.72	8.54	161.7984	72.9316	88.8668	13.8829527
438.3	224.7	213.6	12.71	8.573	161.5441	73.496329	88.047771	13.93659877
436.4	224.4	212	12.65	8.568	160.0225	73.410624	86.611876	13.92847058
412.1	224.7	187.4	12.49	8.54	156.0001	72.9316	83.0685	13.8829527
411.1	224.4	186.7	12.46	8.568	155.2516	73.410624	81.840976	13.92847058
438.7	222.3	216.4	12.73	8.977	162.0529	80.586529	81.466371	14.59335672
440.6	222.6	218	12.74	9	162.3076	81	81.3076	14.63074641
439.6	222.3	217.3	12.75	9.039	162.5625	81.703521	80.858979	14.69414631
410.5	225.7	184.8	12.39	8.542	153.5121	72.965764	80.546336	13.88620398
412.6	224.7	187.9	12.3	8.573	151.29	73.496329	77.793671	13.93659877
412.1	226	186.1	12.24	8.54	149.8176	72.9316	76.886	13.8829527

411	225.7	185.3	12.24	8.583	149.8176	73.667889	76.149711	13.95285516
414.3	222.6	191.7	12.46	9	155.2516	81	74.2516	14.63074641
412.6	223.6	189	12.4	8.969	153.76	80.442961	73.317039	14.58035162
413.2	222.3	190.9	12.44	9.039	154.7536	81.703521	73.050079	14.69414631
412.7	222.3	190.4	12.34	8.977	152.2756	80.586529	71.689071	14.59335672
354.6	226	128.6	11.54	8.54	133.1716	72.9316	60.24	13.8829527
354	224.7	129.3	11.51	8.54	132.4801	72.9316	59.5485	13.8829527
353.4	224.7	128.7	11.52	8.573	132.7104	73.496329	59.214071	13.93659877
353.5	225.7	127.8	11.24	8.542	126.3376	72.965764	53.371836	13.88620398
338.9	224.7	114.2	11.22	8.54	125.8884	72.9316	52.9568	13.8829527
354.2	223.6	130.6	11.54	8.969	133.1716	80.442961	52.728639	14.58035162
352.3	224.4	127.9	11.22	8.568	125.8884	73.410624	52.477776	13.92847058
353	225.7	127.3	11.23	8.583	126.1129	73.667889	52.445011	13.95285516
353.5	222.3	131.2	11.53	8.977	132.9409	80.586529	52.354371	14.59335672
339.2	226	113.2	11.17	8.54	124.7689	72.9316	51.8373	13.8829527
353	222.3	130.7	11.52	9.039	132.7104	81.703521	51.006879	14.69414631
339.4	224.7	114.7	11.15	8.573	124.3225	73.496329	50.826171	13.93659877
338.6	224.4	114.2	11.02	8.568	121.4404	73.410624	48.029776	13.92847058
338.5	225.7	112.8	10.96	8.542	120.1216	72.965764	47.155836	13.88620398
339	225.7	113.3	10.99	8.583	120.7801	73.667889	47.112211	13.95285516
354.6	222.6	132	11.29	9	127.4641	81	46.4641	14.63074641
339.5	222.3	117.2	11.21	8.977	125.6641	80.586529	45.077571	14.59335672
339.9	223.6	116.3	11.18	8.969	124.9924	80.442961	44.549439	14.58035162
340	222.3	117.7	11.12	9.039	123.6544	81.703521	41.950879	14.69414631
340.3	222.6	117.7	10.98	9	120.5604	81	39.5604	14.63074641
							Average:	14.1968635

Table 10: Readout noise for blue filter

B Magnitudes and Extinction Coefficients of Star 3 and Star 4

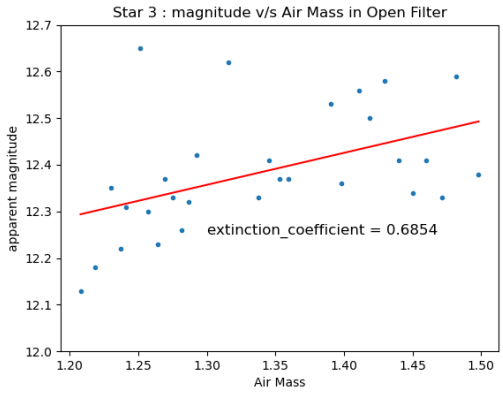

(a) Extinction coefficient in open filter

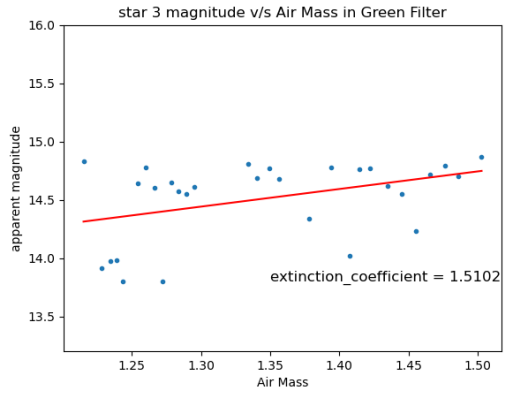

(b) Extinction coefficient in green filter

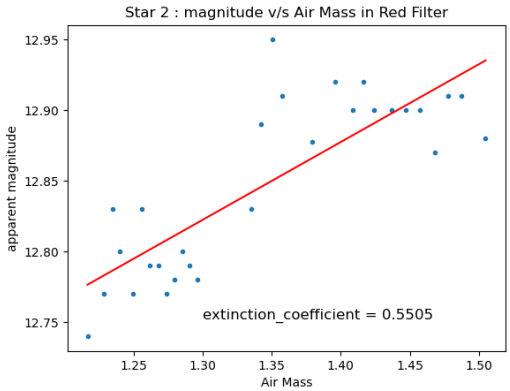

(c) Extinction coefficient in red filter

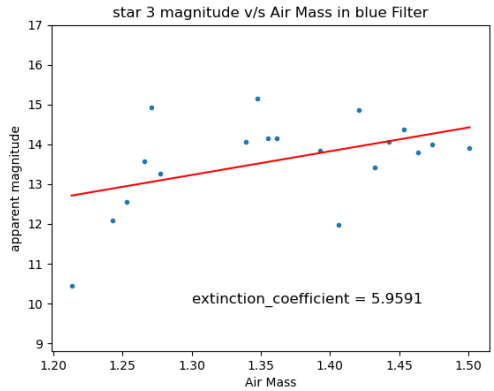

(d) Extinction coefficient in blue filter

Figure 24: Extinction coefficient in different filters for star 3

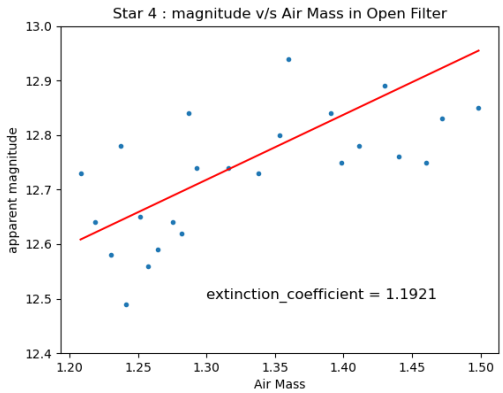

(a) Extinction coefficient in open filter

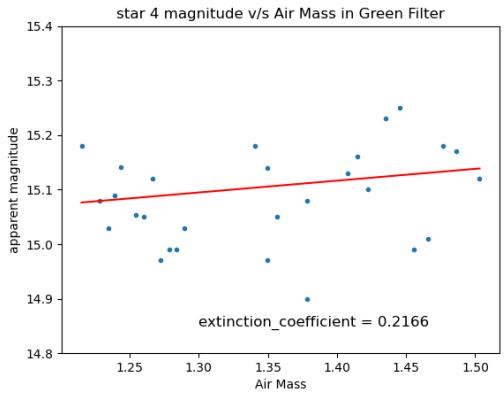

(b) Extinction coefficient in green filter

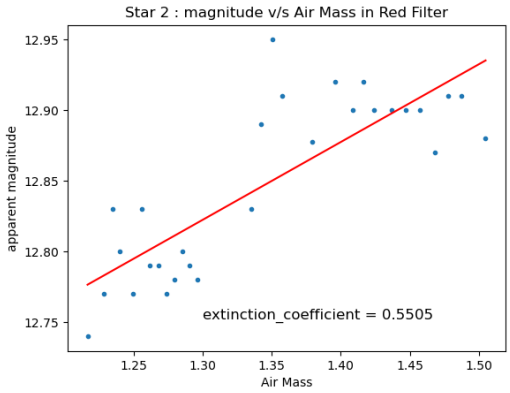

(c) Extinction coefficient in red filter

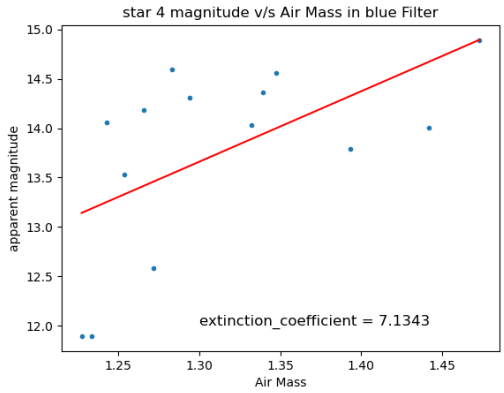

(d) Extinction coefficient in blue filter

Figure 25: Extinction coefficient in different filters for star 4

Filters	**Extinction Coefficient**	**Instrumental Magnitude**
open	0.6854	11.466 ± 0.021
green	1.510	12.4781 ± 0.023
red	1.1333	13.211 ± 0.013
blue	0.2166	5.483 ± 0.009.

Table 11: STAR 3 : V647 TAURI

Filters	Extinction Coefficient	Instrumental Magnitude
open	1.1921	11.1684 ± 0.015
green	0.3061	12.291 ± 0.021
red	0.5317	14.297 ± 0.071
blue	7.1343	4.386 ± 0.043

Table 12: STAR 4 : HD 23608

C CCDSOFT

The following is the screenshot of the software used to obtain the CCD images from the telescope.

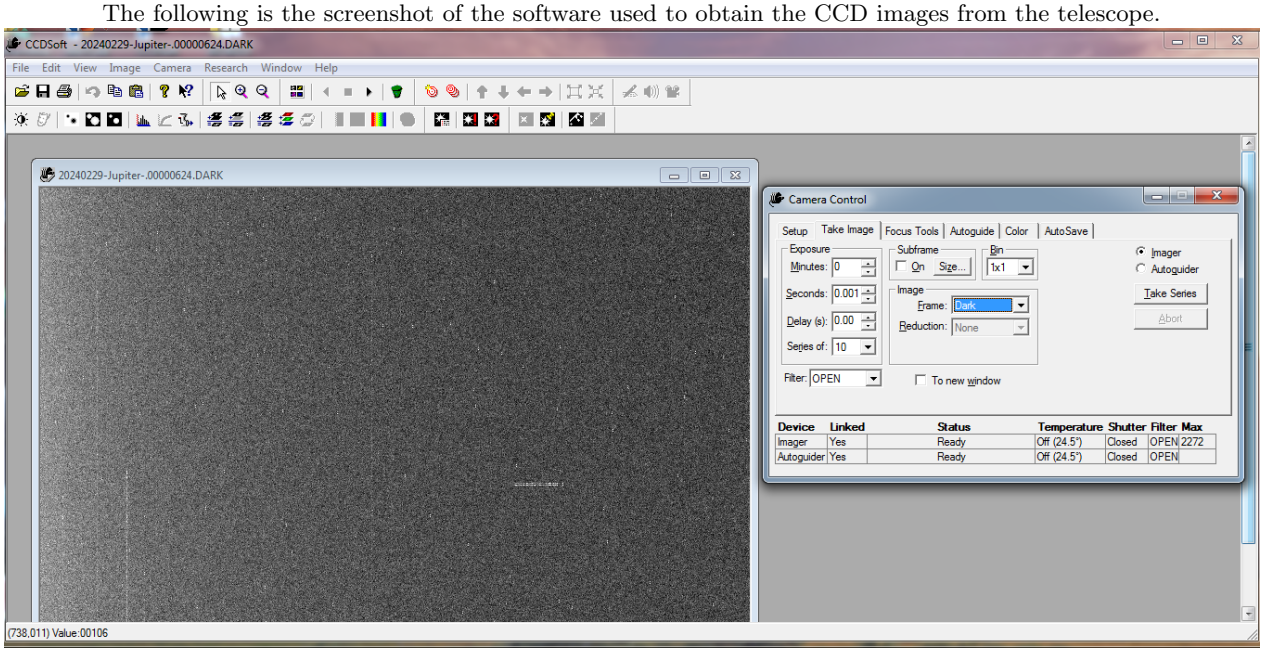

D Log File

OBSERVING LOG

2024

11" Celestron Telescope, Department of Physics and Astrophysics, University of Delhi

Program :
Date : 29/02/2024
Observer's Name : Nitesh

Run	Frame	Object	Band	Time of Observation	Exposure	Comments.
0-49	Light Blue	Jupiter	Blue	8:08 PM	0.001s	—
50-99	Light	"	B	8:10	0.001s	—
100-199	Light	Jupiter	Green	8:12	0.001s	—
200-299	Light	Jupiter	Red	8:17	0.001s	—
300-399	"	"	Blue	8:22	0.001s	—
400-499	"	"	Green	8:26	0.001s	—
500-599	"	"	Red	8:31	0.001s	—
600-699	"	"	OPEN	8:36	0.001s.	About 4 saturated images.
609-614	Bias	"	open	8:37	0.000s	—
615-624	Dark	"	open	8:38	0.001s	—

Program :
Date : 11-03-2024
Observer's Name : Shahana Saifi

Run	Frame	Object	Band	Time of observation	Exposure	Comments
0-4	Flat-Field		Open	6:43	0.01	
5-9	"		Blue	6:44	0.01	Not saved
10-14	"		Green	6:44	0.01	
15-19	"		Red	6:44	0.01	
0-4	"		Red	6:47	0.01	
5-9	"		Green	6:47	0.01	
10-14	"		Blue	6:47	0.01	
15-19	"		Open	6:47	0.01	
20-24	"		Red	6:48	0.02	
25-29	"		Green	6:48	0.02	
30-34	"		Blue	6:49	0.02	
35-39	"		Open	6:49	0.02	
40-44	"		Red	6:49	0.05	
45-49	"		Green	6:50	0.05	
50-54	"		Blue	6:50	0.05	
55-59	"		Open	6:50	0.05	
60-64	"		Red	6:52	0.10	
65-69	"		Green	6:52	0.1	
70-74	"		Blue	6:52	0.1	
75-79	"		Open	6:53	0.1	
80-84	"		Red	6:53	0.2	
85-89	"		Green	6:54	0.2	
90-94	"		Blue	6:54	0.2	
95-99	"		Open	6:54	0.2	
100-104	"		Red	6:55	0.6	

Run	Frame	Object	Band	Time of Observation	Exposure	Comments
105-109	Flat field		Green	6:55	0.5	
110-114	"		Blue	6:56	0.5	
115-119	"		Open	6:56	0.5	
120-124	Bias		open (not needed)	6:57	0.5	
125-1				7:24	1	

Program:
Date: 12.03.2024
Observer's Name:

Run	Frame	Object	Band	Time of Observation	Exposure	Comment
0-2	Light	Pleiades	Open	7:18	0.1	Not ...
3-5	"	"	Blue	7:19	0.1	
6-8	"	"	Blue	7:20	0.2	
9-11	"	"	Blue	7:20	0.5	
12-14	"	"	Green	7:20	0.5	
15-17	"	"	Red	7:21	0.5	
18-20	"	"	Open	7:22	0.1	start
22-24	"	"	Blue	7:24	0.5	
25-27	"		Green	7:24	0.5	
28-30	"		Red	7:25	0.5	
31-33	"		Open	7:25	0.1	
34-36	"		Blue	7:26	0.5	
37-39	"		Green	7:26	0.5	
40-42			Red.	7:27	0.5	
43-45			Open	7:27	0.1	
46-48			Blue	7:27	0.5	
49-51			Green	7:28	0.5	
52-54			Red	7:28	0.5	
55-57			Open	7:28	0.1	
58-60			Blue	7:29	0.5	
61-63			Green	7:29	0.5	
64-66			Red	7:30	0.5	
67-69			Open	7:31	0.1	
70-72			Blue	7:32	0.5	
73-75			Green	7:32	0.5	
76-78			Red	7:32	0.5	
79-81			Open	7:33	0.1	
82-84			Blue	7:33	0.5	
85-87			Green	7:34	0.5	

Run	Frame	Object	Band	Time of Observation	Exposure	Comments
88-90	Light	Pleiades.	~~Open~~ Red	7:34	0.5	
91-93	"	"	Open	7:35	0.1	
94-96	"	"	Blue	7:35	0.5	
97-99	"	"	Green	7:35	0.5	
100-102	"	"	Red	7:36	0.5	
103-105	"	"	Open	7:36	0.1	
106-108	"	"	Blue	7:36	0.5	
109-111	"	"	Green	7:37	0.5	
112-114	"	"	Red	7:37	0.5	
115-117	"	"	Open	7:37	0.1	
118-120	"	"	Blue	7:38	0.5	
121-123	"	"	Green	7:38	0.5	
124-126	"	"	Red	7:39	0.5	
127-129	"	"	Open	7:39	0.1	
130-132	"	"	Blue	7:39	0.5	
133-135	"	"	Green	7:40	0.5	
136-138	"	"	Red	7:40	0.5	
139-141	"	"	Open	7:40	0.1	
142-144	"	"	Blue	7:41	0.5	
145-147	"	"	Green	7:41	0.5	
148-150	"	"	Red	7:42	0.5	
151-153	"	"	Open	7:42	0.1	
154-156	"	"	Blue	7:42	0.5	
157-159	"	"	Green	7:43	0.5	
160-162	"	"	Red	7:43	0.5	
163-164	"	"	Open	7:46	0.1	delete this ~~abort~~
~~165-167~~	"	"	~~Blue~~ Open		0.5	
			~~Green~~ blue		0.5	
165			~~red~~ green		~~0.5~~	abort.

Run	Frame	Object	Band	Time of Observation	Exposure	Comments
166-168	Light	Pleiades	Open	7:47	0.1	
169-171	"	"	Blue	7:51	0.5	
172-174	"	"	Green	7:52	0.5	
175-177	"	"	Red	7:52	0.5	
178-180	"	"	Open	7:52	0.1	
181-183	"	"	Blue	7:53	0.5	
184-186	"	"	Green	7:53	0.5	
187-189	"	"	Red	7:53	0.5	
190-192	"	"	Open	7:54	0.1	
193-195	"	"	Blue	7:55	0.5	
196-198	"	"	Green	7:55	0.5	
199-201	"	"	Red	7:55	0.5	
202-204	"	"	Open	7:56	0.1	
205-207	"	"	Blue	7:56	0.5	
208-210	"	"	Green	7:57	0.5	
211-213	"	"	Red	7:57	0.5	
214-216	"	"	Open	7:57	0.1	
217-219	"	"	Blue	7:58	0.5	
220-222	"	"	Green	8:01	0.5	
223-225	"	"	Red	8:01	0.5	
226-228	"	"	Open	8:03	0.1	
229-231	"	"	Blue	8:04	0.5	
232-234	"	"	Green	8:04	0.5	
235-237	"	"	Red	8:04	0.5	
238-240	"	"	Open	8:05	0.1	
241-243	"	"	Blue	8:06	0.5	
244-246	"	"	Green	8:07	0.5	
247-249	"	"	Red	8:07	0.5	
250-252	"	"	Open	8:07	0.1	
253-255	"	"	Blue	8:08	0.5	

Run	Frame	Object	Band	Time of Observation	Exposure	Comments
256-258	"	"	Green	8:08	0.5	
259-261	"	"	Red	8:08	0.5	
262-264	"	"	Open	8:09	0.1	
265-267	"	"	Blue	8:09	0.5	
268-270	"	"	Green	8:09	0.5	
271-273	"	"	Red.	8:10.	0.5	
274-276	"	"	Open	8:11	0.1	
277-279	"	"	Blue	8:11	0.5	
280-282	"	"	Green	8:12	0.5	
283-285	"	"	Red.	8:12	0.5	
286-288	"	"	Open	8:12	0.1	
289-291	"	"	Blue	8:13	0.5	
292-294	"	"	Green	8:13	0.5	
295-297	"	"	Red	8:14	0.5	
298-300	"	"	Open	8:14	0.1	
301-303	"	"	Blue	8:15	0.5	
304-306	"	"	Green	"	0.5	
307-309	"	"	Red	8:16	0.5	
310-312	"	"	Open	"	0.1	
313-315	"	"	Blue	8:17	0.5	
316-318	"	"	Green	8:17	0.5	
319-321	"	"	Red.	8:17	0.5	
322-324	"	"	Open	8:18	0.1	
325-327	"	"	Blue	8:18	0.5	
328-330	"	"	Green	8:19	0.5	
331-333	"	"	Red.	8:19	0.5	
334-336	"	"	Open	8:20	0.1	
337-339	"	"	Blue	8:20	0.5	
340-342	"	"	Green	8:20.	0.5	
343-345	"	"	Red	8:21	0.5	

Run	Frame	Object	Band	time of observation	Exposure (seconds)	Comments
346-348	Light	Pleides	open	8:22	0.1	
349-351	"	"	Blue	8:23	0.5	
352-354	"	"	Green	8:23	0.5	
355-357	"	"	Red	8:23	0.5	
0-9	Light	Orion	Red	8:36	1.5	
10-19	"	Nebula	Green	8:36	1.5	
20-29	"	"	Blue	8:37	1.5	
30-39	"	"	open	8:38	1.5	

E Astrophotography (Image Reduction)

The following are the images of Jupiter and Orion Nebula taken using our observatory telescope and further processed into colored images using Siril. Please note that the rotation effects were not corrected.

Figure 26: Jupiter as viewed from Department of Physics and Astrophysics, University of Delhi

Figure 27: Orion Nebula as viewed from Department of Physics and Astrophysics, University of Delhi

Bibliography

[1] https://www.researchgate.net/profile/Ali-Tavackolimehr/publication/332392902_Handbook_of_CCD_Astronomy/links/5cb134f6299bf1209762473d/Handbook-of-CCD-Astronomy.pdf

[2] https://astro.uni-bonn.de/~sysstw/lfa_html/iraf/noao.nproto.findgain.html

[3] http://www.astrosurf.com/buil/isis/noise/result.htm

[4] https://cdn.technologynetworks.com/ep/pdfs/characterization-of-a-ccd-camera-for-astro pdf

[5] Tutorials: Basic Image Reduction with IRAF by Kaustubh Vaghmare

[6] Stellar Photometry Using IRAF - W. E. Harris (September 2008)

[7] https://iraf.net/irafdocs/apuser.pdf

[8] https://docs.astropy.org/en/stable/time/

[9] https://lovethenightsky.com/fast-and-slow-telescopes/

[10] Telescope Celestron CGE1100 Instruction Manual

[11] SBIG ST7XME Instruction Manual

[12] Filter Wheel IFW Technical Manual